



## Original article

A class of novel *N*-isoquinoline-3-carbonyl-L-amino acid benzylesters: Synthesis, anti-tumor evaluation and 3D QSAR analysisMeiqing Zheng<sup>a</sup>, Yifan Yang<sup>a</sup>, Ming Zhao<sup>a,\*\*</sup>, Xiaoyi Zhang<sup>a</sup>, Jianhui Wu<sup>a</sup>, Gong Chen<sup>b,\*\*\*</sup>, Li Peng<sup>a</sup>, Yuji Wang<sup>a</sup>, Shiqi Peng<sup>a,\*</sup><sup>a</sup> College of Pharmaceutical Sciences, Capital Medical University, No. 10, Xitoutiao, You An Men, Beijing 100069, PR China<sup>b</sup> Department of chemistry, The Pennsylvania state University, 104 chemistry Building, University Park, PA 16802, USA

## ARTICLE INFO

## Article history:

Received 29 July 2010

Received in revised form

3 January 2011

Accepted 12 February 2011

Available online 22 February 2011

## Keywords:

*N*-Isoquinoline-3-carbonylamino acid

benzylester

Intercalator

Anti-tumor

3D QSAR

Membrane permeability

## ABSTRACT

Isoquinoline-3-carboxylic acid (**2**) was modified with amino acid benzylesters and 18 novel *N*-isoquinoline-3-carbonylamino acid benzylesters (**3a–r**) were provided. The IC<sub>50</sub> values of **3a–r** against the proliferation of HL-60 and Hela cells were less than  $1 \times 10^{-8}$  M and  $6 \times 10^{-7}$  M, respectively. On S180 mice model 100 μmol/kg of **3a–r** effectively inhibited the growth of the tumors. Using MFA based Cerius<sup>2</sup> QSAR module, two equations ( $r$ , 0.989 and 0.987) were established to correlate the structure with the *in vitro* and *in vivo* activities. The benefit of this modification was supported with both the *in vitro* membrane permeation test and the *in vivo* anti-tumor assay. The *in vitro* membrane permeability of *N*-isoquinoline-3-carbonyl-L-threonine benzylester (**3n**) and *N*-isoquinoline-3-carbonyl-L-leucine benzylester (**3q**) was 2.5 fold higher than that of **2**, and the *in vivo* anti-tumor activity of **3n, q** was 4.4-fold higher than that of **2**.

© 2011 Elsevier Masson SAS. All rights reserved.

## 1. Introduction

In spite of the total progress in diagnosis and therapy, cancer is still one of the major human diseases and causes great suffering and financial loss worldwide. To improve the chemotherapy in the past decades continuous efforts have been made for discovering new anti-tumoral leads and a great diversity of substances has been explored. Among the discovered substances, isoquinoline derivatives are capable of acting on cell-cycle [1–3] and farnesoid × receptor [4], inhibit IGF to IGF-binding proteins [5], function as redox-cycler [6–8], and are involved in the mutant B-Raf pathway and the pathway that relate to extracellular signal-regulated kinase/c-Jun N-terminal kinase [9,10]. Besides, isoquinoline derivatives are the inhibitors of a number of cancer related enzymes including inosine 5'-monophosphate dehydrogenase [11], Pfmrk [12], P-glycoprotein [13–15], kinase B/Akt [16], cyclin-dependent kinase 4 [17], topoisomerase I [18–27], TRPV1 [28], IkB

kinase-β [29], caspase-3 [30], and mammalian sterile 20 kinase [31]. Alternately, via alkylation toward the minor groove of DNA, generating minimum intermediates or intercalating into the double strands of the DNA isoquinoline derivatives can directly act on the DNA of cancer cells [32–39]. On the other hand, isoquinoline-3-carboxylic acid and derivatives have been explored to be the rigid mimic of tyrosine conformation in the opioid ligand–receptor complex [40], the reverse turn mimetics [41], the antagonists of ampa receptor [42], the inhibitors on the binding of IGF to IGF-binding proteins [43], and the antagonists of AT1 receptor [44]. However, so far no anti-tumoral isoquinoline-3-carboxylic acid derivatives were disclosed. Due to our ongoing interest in the discovery of isoquinolines functioning in the therapy of leukemia or cervical carcinoma, the structural correlation of isoquinoline-3-carboxylic acid with 1-methyl-β-carboline-3-carboxylic acid, the increase of the *in vitro* anti-proliferation activity resulted from the structure-simplification from 1-methyl-β-carboline-3-carboxylic acid to isoquinoline-3-carboxylic acid (Fig. 1), and the benzyl ester of 1-methyl-β-carboline-3-carboxylic acid having higher *in vitro* anti-proliferation activity than the acid and methyl ester [45,46], this paper describes the preparation, the *in vitro* anti-proliferation of HL-60 and Hela cell lines, the *in vivo* anti-tumor activities, and the 3D QSAR analysis of 18 novel *N*-isoquinoline-3-carbonyl-L-amino acid benzylesters.

\* Corresponding author. Tel./fax: +86 10 8391 1528.

\*\* Corresponding author. Tel./fax: +86 10 8280 2482.

\*\*\* Corresponding author. Tel.: +1 (814) 867 2590; fax: +1 (814) 863 5319.

E-mail addresses: [mingzhao@mail.bjmu.edu.cn](mailto:mingzhao@mail.bjmu.edu.cn) (M. Zhao), [guc11@psu.edu](mailto:guc11@psu.edu) (G. Chen), [speng@mail.bjmu.edu.cn](mailto:speng@mail.bjmu.edu.cn) (S. Peng).

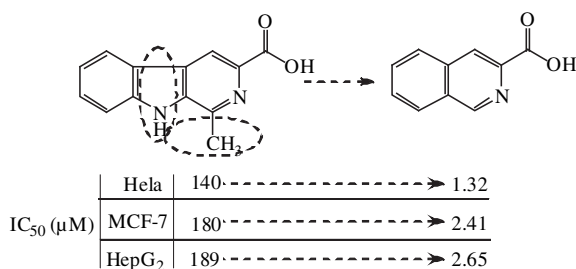


**Fig. 1.** Structural correlation and comparison of the *in vitro* anti-proliferation activities of  $\beta$ -carboline-3-carboxylic acid (data from Ref. [45]) and isoquinoline-3-carboxylic acid (data from the preliminary assays of this paper).

## 2. Results and discussion

### 2.1. Synthesis of *N*-isoquinoline-3-carbonyl-*L*-amino acid benzylesters **3a–r**

The preparation of *N*-isoquinoline-3-carbonylamino acid benzylesters (**3a–r**) was carried out according to the three-step-route of Scheme 1. In the first step, via Pictet–Spengler condensation *L*-Phe was converted into 3*S*-1,2,3,4-tetrahydroisoquinoline-3-carboxylic acid (**1**, 84% yield). In the second step, **1** was oxidized with  $\text{KMnO}_4$  and isoquinoline-3-carboxylic acid **2** was obtained in 83% yield. In the third step, amino acid benzylesters were introduced into **2** by the DCC/HOBt/*N*-methylmorpholine (NMM) procedure to give *N*-isoquinoline-3-carbonyl-*L*-amino acid benzylesters (**3a–r**, 53–87% yield). The mild condition and the acceptable yields suggest that this three-step-route is suitable for preparing these novel compounds.

### 2.2. *In vitro* anti-proliferation activity of **3a–r**

Following the 3-(4,5-dimethylthiazol-2-yl)-2,5-diphenyltetrazolium bromide (MTT) method, the *in vitro* anti-proliferation assays were carried out on 96 microtiter plates, and the  $\text{IC}_{50}$  values of **3a–r** inhibiting the growth of HL-60 and Hela cells were

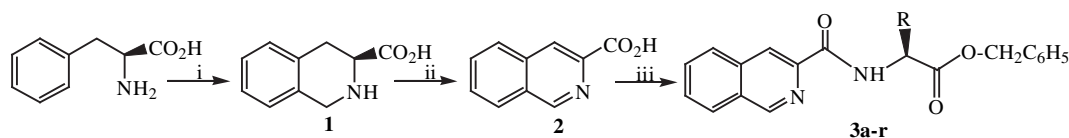
determined. The results are listed in Table 1. The  $\text{IC}_{50}$  values of **3a–r** inhibiting the growth of HL-60 cells ranged from 44.50 to 99.94 nM, while the  $\text{IC}_{50}$  values of **3a–r** inhibiting the growth of Hela cells ranged from 87.74 to 507.94 nM. It was explored that for both HL-60 and Hela cells **3b,e,g,n,q** consistently exhibited desirable inhibition activity.

### 2.3. *In vivo* anti-tumor activity of **3a–r**

Following a general procedure the *in vivo* assay was carried out. In the assays the tumor weight of the treated S180 mice was used to express the activity of **3a–r** (100  $\mu\text{mol/kg/day}$  in 0.2 ml of NS) with 0.2 ml of normal saline (NS) as the negative control and cytarabine (100  $\mu\text{mol/kg/day}$  in 0.2 ml of NS) as the positive control. The intraperitoneal treatment was carried out for 7 consecutive days. The results are listed in Table 2. The data indicate that the tumor weights of **3a–r** treated mice range from 0.821 to 1.588 g and are significantly lower than that of NS treated mice (1.802 g,  $p < 0.01$ ), which suggests that at this dose they possess anti-tumor activity. In addition, the anti-tumor efficacy of 100  $\mu\text{mol/kg/day}$  of **3n, q** is substantially equal to that of 100  $\mu\text{mol/kg/day}$  of cytarabine (0.814 g,  $p > 0.05$ ), and **3a, e, g** exhibit desirable *in vivo* anti-tumor efficacy. Therefore in both *in vitro* and *in vivo* assays **3e, g, n, q** consistently give desirable activity. It was also noticed that the *in vitro* efficacy did not match the *in vivo* efficacy. It has been well known that the *in vitro* efficacy does not match with the *in vivo* efficacy is not a rare phenomena. Perhaps the absorption, delivery, distribution and metabolism are partly responsible for the mentioned phenomena of **3a–r**.

### 2.4. Dose-dependence of the oral anti-tumor activity of **3g, n, q**

The oral administration of **3g, n, q** was observed at the doses of 1, 10 and 100  $\mu\text{mol/kg}$  to see the possible dose-dependent *in vivo* anti-tumor response of S180 mice. The data are listed in Table 3, and demonstrate that the tumor weight of the treated mice is progressively increased with dose decrease. Therefore, oral **3g, n, q** dose-dependently inhibit the tumor growth of the treated S180 mice. This also suggests that **3a–r** should allow oral administration.



**Scheme 1.** Synthetic route of *N*-isoquinoline-3-carbonyl-*L*-amino acid benzylesters. (i)  $\text{HCHO}$  and  $\text{HCl}$ ; (ii)  $\text{DMF}$  and  $\text{KMnO}_4$ ; (iii)  $\text{L-AA-OCH}_2\text{C}_6\text{H}_5$ ,  $\text{DCC}$  and  $\text{NMM}$ ; In **3a**  $\text{R} = \text{CH}_3$ , **3b**  $\text{R} = \text{CH}(\text{CH}_3)_2$ , **3c**  $\text{R} = \text{CH}(\text{CH}_3)\text{CH}_2\text{CH}_3$ , **3d**  $\text{R} = \text{indol-3-ylmethyl}$ , **3e**  $\text{R} = \text{CH}_2\text{OH}$ , **3f**  $\text{R} = 4\text{-hydroxybenzyl}$ , **3g**  $\text{R} = \text{cyclobutylamino}$ , **3h**  $\text{R} = \text{CH}_2\text{CH}_2\text{CONH}_2$ , **3i**  $\text{R} = \text{imidazol-4-ylmethylene}$ , **3j**  $\text{R} = 4\text{-aminobutyl-1-yl}$ , **3k**  $\text{R} = \text{benzyloxycarbonylmethyl}$ , **3l**  $\text{R} = 2\text{-benzyloxycarbonylethyl-1-yl}$ , **3m**  $\text{R} = \text{benzyl}$ , **3n**  $\text{R} = \text{CH}(\text{OH})\text{CH}_3$ , **3o**  $\text{R} = \text{CH}_2\text{CH}_2\text{SCH}_3$ , **3p**  $\text{R} = \text{H}$ , **3q**  $\text{R} = \text{CH}_2\text{CH}(\text{CH}_3)_2$ , **3r**  $\text{R} = \text{CH}_2\text{CONH}_2$ .

**Table 1**

The  $\text{IC}_{50}$  values of **3a–r** inhibiting proliferation of HL-60 and Hela cells.

Compound	$\text{IC}_{50}$ ( $\bar{X} \pm \text{SD}$ nM, $n = 6$ )		Compound	$\text{IC}_{50}$ ( $\bar{X} \pm \text{SD}$ nM, $n = 6$ )	
	HL-60	Hela		HL-60	Hela
<b>3a</b>	84.84 $\pm$ 5.81	154.46 $\pm$ 12.62	<b>3k</b>	73.96 $\pm$ 4.91	411.30 $\pm$ 15.31
<b>3b</b>	78.94 $\pm$ 6.64	118.29 $\pm$ 5.20	<b>3l</b>	83.62 $\pm$ 5.72	213.61 $\pm$ 16.52
<b>3c</b>	96.35 $\pm$ 5.31	185.42 $\pm$ 12.34	<b>3m</b>	91.79 $\pm$ 9.52	151.00 $\pm$ 10.81
<b>3d</b>	66.12 $\pm$ 9.72	396.46 $\pm$ 19.47	<b>3n</b>	62.25 $\pm$ 5.64	98.69 $\pm$ 9.74
<b>3e</b>	70.39 $\pm$ 9.16	134.65 $\pm$ 13.12	<b>3o</b>	44.88 $\pm$ 6.93	308.75 $\pm$ 15.56
<b>3f</b>	99.94 $\pm$ 7.91	507.94 $\pm$ 15.41	<b>3p</b>	57.35 $\pm$ 7.63	195.43 $\pm$ 10.31
<b>3g</b>	53.42 $\pm$ 9.44	87.74 $\pm$ 13.84	<b>3q</b>	72.76 $\pm$ 6.72	110.55 $\pm$ 8.94
<b>3h</b>	44.50 $\pm$ 5.92	180.67 $\pm$ 12.42	<b>3r</b>	86.94 $\pm$ 6.81	216.31 $\pm$ 14.33
<b>3i</b>	87.56 $\pm$ 6.16	263.43 $\pm$ 15.24	<b>2</b>	948.52 $\pm$ 12.4	1320.15 $\pm$ 16.8
<b>3j</b>	68.24 $\pm$ 7.64	195.67 $\pm$ 10.38			

**Table 2**  
Effect of intraperitoneal **3a–r** on tumor growth of treated S180 mice.

Compound <sup>a</sup>	Tumor weight	% Inhibition	Compound <sup>a</sup>	Tumor weight	%Inhibition
<b>3a</b>	1.071 ± 0.086 <sup>b</sup>	40.6 ± 4.3	<b>3l</b>	1.347 ± 0.061 <sup>b</sup>	25.2 ± 3.8
<b>3b</b>	1.266 ± 0.094 <sup>b</sup>	29.7 ± 2.3	<b>3m</b>	1.260 ± 0.204 <sup>b</sup>	30.1 ± 3.7
<b>3c</b>	1.425 ± 0.085 <sup>b</sup>	20.9 ± 3.1	<b>3n</b>	0.821 ± 0.043 <sup>c</sup>	54.4 ± 5.6
<b>3d</b>	1.137 ± 0.105 <sup>b</sup>	36.9 ± 2.6	<b>3o</b>	1.088 ± 0.164 <sup>b</sup>	39.6 ± 2.8
<b>3e</b>	1.074 ± 0.216 <sup>b</sup>	40.4 ± 3.8	<b>3p</b>	1.511 ± 0.041 <sup>b</sup>	16.1 ± 2.1
<b>3f</b>	1.297 ± 0.103 <sup>b</sup>	28.0 ± 3.0	<b>3q</b>	0.953 ± 0.126 <sup>c</sup>	47.1 ± 5.8
<b>3g</b>	1.001 ± 0.050 <sup>b</sup>	44.5 ± 5.2	<b>3r</b>	1.140 ± 0.151 <sup>b</sup>	36.7 ± 4.5
<b>3h</b>	1.588 ± 0.102 <sup>b</sup>	11.9 ± 2.4	<b>2</b>	1.595 ± 0.300	11.5 ± 3.8
<b>3i</b>	1.364 ± 0.234 <sup>b</sup>	24.3 ± 3.1	Cytarabine	0.814 ± 0.066 <sup>b</sup>	54.8 ± 14.5
<b>3j</b>	1.493 ± 0.078 <sup>b</sup>	40.6 ± 4.3	NS	1.802 ± 0.063	0
<b>3k</b>	1.127 ± 0.114 <sup>b</sup>	37.5 ± 4.1			

<sup>a</sup> Tumor weight is represented by  $\bar{X} \pm SD$  g; inhibition is represented by  $\bar{X} \pm SD\%$ ; NS (normal saline) = vehicle;  $n = 12$ ; Cytarabine, **2** and **3a–r**: dose = 100  $\mu\text{mol/kg}$ .

<sup>b</sup> Compared to NS  $p < 0.01$ .

<sup>c</sup> Compared to NS  $p < 0.01$  and to cytarabine  $p > 0.05$ .

### 2.5. Neurotoxic and acute toxicity of **3g, n, q** treated healthy mice

Neurotoxic and acute toxicity of the most potent **3g, n, q** was assayed by use of a general procedure on the healthy mice. It was found that during 7-day observation the healthy mice orally receiving 15, 90 and 540 mg/kg of **3g, n, q** exhibited no any neurotoxic behavior, such as tremor, twitch, jumping, tetanus, as well as supination. On the 7th day the necropsy findings of the mice gave also no apparent changes in their organs. These observations suggest that **3g, n, q** are low toxic agents. Besides, even up to 540 mg/kg of dose the treated healthy mice occurred no death. This observation suggests that the LD<sub>50</sub> value of **3g, n, q** is more than 540 mg/kg. At the dose of 540 mg/kg the treated mice having 100% survival and without neurotoxic behavior implies that **3g, n, q** are safe anti-tumor leads.

### 2.6. 3D QSAR analysis of **3a–r**

To understand the dependence of the *in vitro* and *in vivo* anti-tumor activity of **3a–r** upon their structure, the corresponding 3D QSAR analysis was performed. Training set (**3a–o**)/test set (**3p–r**) selections were done manually such that they populate the wide range of anti-tumor activity in similar proportion. In the analysis, the alignment, MFA based Cerius<sup>2</sup> QSAR module of **3a–r** and the electrostatic and steric environments of them within the grid with 3D points of the equation were involved.

#### 2.6.1. Alignment of **3a–r**

For establishing the valid 3D-QSAR models, a proper alignment procedure of **3a–r** was practiced using the target model align strategy in the align module within Cerius<sup>2</sup>. Based on the assumption that each structure of **3a–r** exhibits activity at the same binding site of the receptor, they were aligned in a pharmacological

active orientation. To obtain a consistent alignment, isoquinoline ring was selected as the template for superposing **3a–r**. The method used for performing the alignment was the maximum common subgraph (MCS) [47]. MCS looks at molecules as points and lines, and uses the techniques out of graph theory to identify the patterns. Then MCS finds the largest subset of atoms in isoquinoline ring that shared by **3a–r**. This subset was used for the alignment. A rigid fit of atom pairings was performed to superimpose each structure onto the target model isoquinoline ring. Stereoview of aligned **3a–r** is shown in Fig. 2. The alignment stereoview explores that to superimpose onto isoquinoline ring the amino acid residue of each structure has to take individual conformation. As seen in Tables 2 and 3 this individual conformation of amino acid residue corresponds an individual anti-tumor activity.

#### 2.6.2. MFA based Cerius<sup>2</sup> QSAR module of **3a–o**

Molecular field analysis (MFA) was performed for **3a–o** with the QSAR module of Cerius<sup>2</sup> [48]. A five-step-procedure consisted of generating conformers, energy minimization, matching atoms and

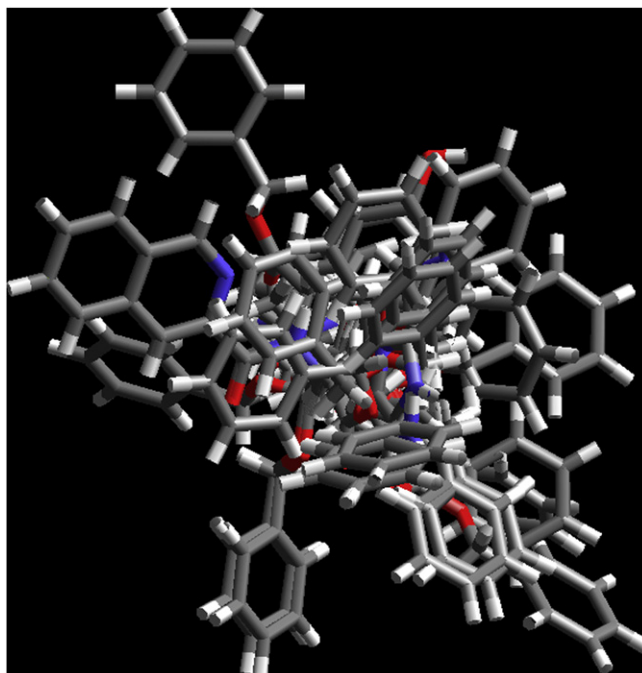


Fig. 2. Alignment stereoview of **3a–r** used for molecular field generation.

**Table 3**  
Effect of different oral doses of **3g, n, q** on tumor growth of treated S180 mice<sup>a</sup>.

Compound	Tumor weight		
	1 $\mu\text{mol/kg}$	10 $\mu\text{mol/kg}$	100 $\mu\text{mol/kg}$
<b>3g</b>	1.661 ± 0.076 <sup>b</sup>	1.243 ± 0.181 <sup>c</sup>	1.021 ± 0.044 <sup>d</sup>
<b>3n</b>	1.315 ± 0.078 <sup>b</sup>	1.184 ± 0.167 <sup>c</sup>	0.802 ± 0.043 <sup>d</sup>
<b>3q</b>	1.298 ± 0.094 <sup>b</sup>	1.011 ± 0.085 <sup>c</sup>	0.938 ± 0.117 <sup>d</sup>
NS	1.879 ± 0.127	Cytarabine (100 $\mu\text{mol/kg}$ ): 0.814 ± 0.066 <sup>d</sup>	

<sup>a</sup> Tumor weight is represented by  $\bar{X} \pm SD$ g, NS = vehicle;  $n = 12$ ; cytarabine was intraperitoneally administered.

<sup>b</sup> Compared to NS  $p < 0.01$ .

<sup>c</sup> Compared to NS  $p < 0.01$ , to cytarabine  $p > 0.05$ .

<sup>d</sup> Intraperitoneal injection.

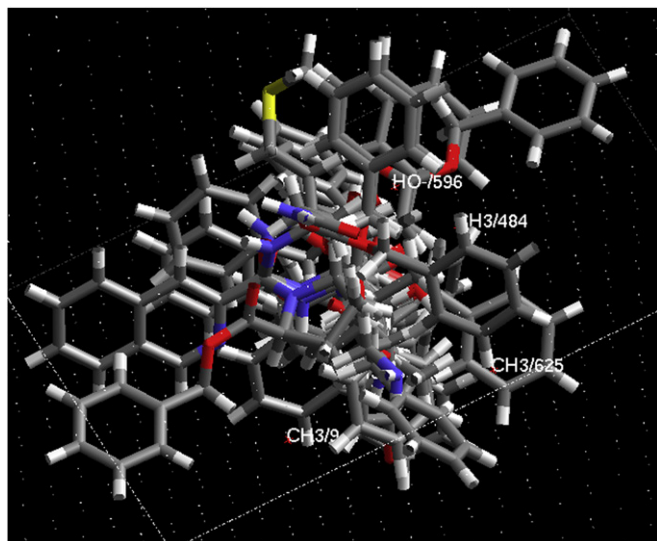


Fig. 3. Steric or electrostatic features of **3a–r** led to increasing or decreasing of anti-proliferation of HL60 *in vitro*.

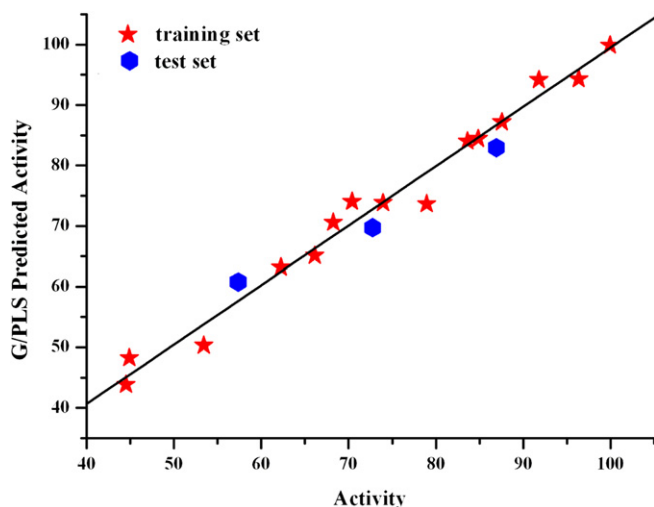


Fig. 4. Graph of tested *in vitro* anti-proliferation activity versus predicted *in vitro* anti-proliferation activity of **3a–r**.

aligning molecules, setting preferences, and regression analysis was automatically practiced in MFA. Molecular electrostatic and steric fields were created by use of proton, methyl and hydroxyl anion as probes, respectively. These fields were sampled at each point of a regularly spaced grid of 1 Å. An energy cutoff of  $\pm 30.0$  kcal/mol

Table 4  
Predict and test *in vitro* anti-proliferation activities of **3p–r**.

Compound	IC <sub>50</sub> (nM)			
	Predict value	Test value	Error	Error%
<b>3p</b>	60.80	57.35	−3.45	−6.0
<b>3q</b>	69.70	72.76	3.06	4.2
<b>3r</b>	82.96	86.94	3.98	4.6

was set for both electrostatic and steric fields. The total grid points generated were 672. Though the spatial and structural descriptors such as dipole moment, polarizability, radius of gyration, number of rotatable bonds, molecular volume, principal moment of inertia, AlogP98, number of hydrogen bond donors and acceptors, and molar refractivity were also considered, only the highest variance holder proton and methyl descriptors were used. Regression analysis was carried out using the genetic partial least squares (G/PLS) method consisting of 50,000 generations with a population size of 100. The number of components was set to 5. Cross-validation was performed with the leave-one-out procedure. PLS analysis was scaled, with all variables normalized to a variance of 1.0.

2.6.2.1. 3D QSAR equation of **3a–o** in terms of inhibiting the proliferation of HL60 *in vitro*. Based on the module, the regions where variations in the steric or electrostatic features of **3a–o** led to the increase or decrease of their *in vitro* inhibition of proliferation of HL60 were specified as Fig. 3. In the MFA model, the activities of **3a–o** inhibiting the proliferation of HL60 in terms of the most relevant descriptors including methyl and hydroxyl anion is expressed with Eq. (1).

$$\text{IC}_{50}(\text{nM}) = 48.06 + 0.68(\text{CH}_3/625) + 0.84(\text{CH}_3/835) + 0.53(\text{CH}_3/944) - 0.63(\text{CH}_3/484) + 0.28(\text{HO}^-/596) \quad (1)$$

The correlation of the activities tested on the *in vitro* proliferation model of HL60 and the activities calculated with Eq. (1) is explained with Fig. 4. In Eq. (1) the data points ( $n$ ), correlation coefficient ( $r$ ) and square correlation coefficient ( $r^2$ ) were 15, 0.989 and 0.978, respectively. These parameters indicate that Eq. (1) is able to predict the *in vitro* activity for **3a–o**.

Eq. (1) contains 4 terms from methyl descriptor and 1 term from hydroxyl anion descriptor. The terms of 0.68 (CH<sub>3</sub>/625), 0.84 (CH<sub>3</sub>/835) and 0.53 (CH<sub>3</sub>/944) have positive coefficients, which means that at these positions small groups will increase the activity, while the term of 0.63 (CH<sub>3</sub>/484) has negative coefficient, which means that at this position large group will increase the activity. The term of 0.28 (HO<sup>−</sup>/596) has positive coefficient, which means that at this position hydrogen bond forming group will decrease the activity.

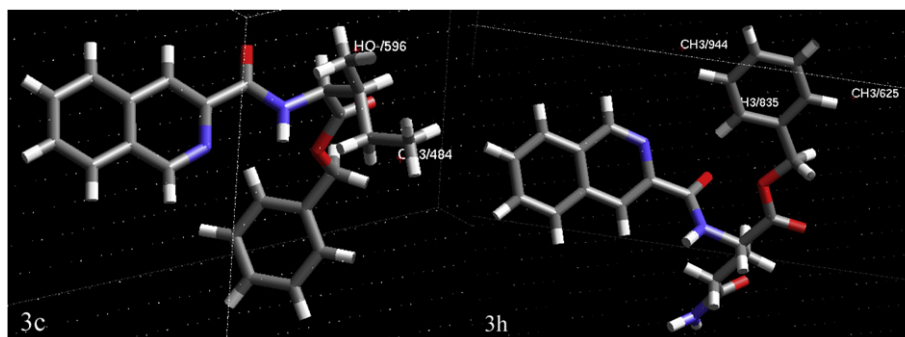


Fig. 5. Electrostatic and environments of **3c** and **3h** within the grid with 3D points of Eq. (1).

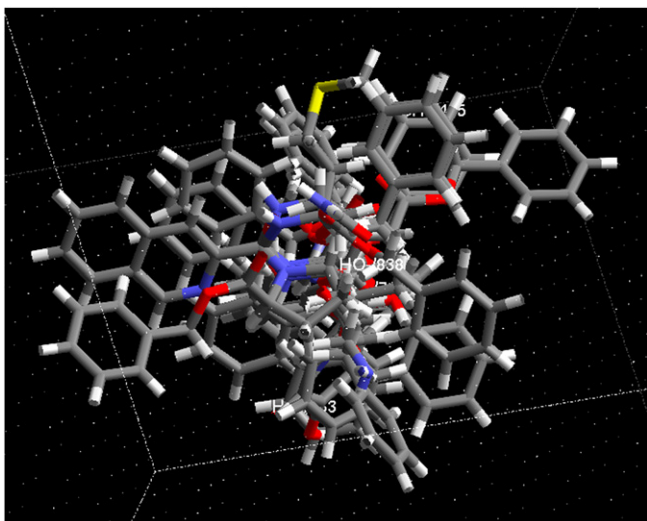


Fig. 6. Steric or electrostatic features of **3a–r** led to increasing or decreasing of anti-tumor activity *in vivo*.

Table 5

Predict and test *in vivo* anti-tumor activities of **3p–r**.

Compound	Tumor weight (g)			
	Predict value	Test value	Error	Error%
<b>3p</b>	1.446	1.511	−0.065	−4.3
<b>3q</b>	1.006	0.953	0.053	5.6
<b>3r</b>	1.130	1.140	−0.01	−0.87

near the region of CH<sub>3</sub>/835, thus it totally has high *in vitro* anti-proliferation activity.

2.6.2.2. Predicting the *in vitro* anti-proliferation activity of **3p–r** with Eq. (1). The predict power of Eq. (1) was demonstrated by comparing the calculated and tested *in vitro* anti-proliferation activity of **3p–r** (Table 4). The correlations of the predict and the test values are also shown in Fig. 4. The results indicate that Eq. (1) rationally gives *in vitro* anti-proliferation activity for **3p–r** and the errors range from −3.45 to 3.98 nM. The calculated activity is so approximate to experimental activity means that Eq. (1) is practical to accurately predict the *in vitro* anti-proliferation activity of isoquinoline-3-carboxyl-L-amino acid benzylesters.

2.6.2.3. 3D QSAR equation of **3a–o** inhibiting tumor growth of treated S180 mice. Based on the module, the regions where variations in the steric or electrostatic features of **3a–r** lead to the inhibition or enhancement of tumor growth of the treated S180 mice were specified as in Fig. 6. In the MFA model, the *in vivo* anti-tumor activity of **3a–o** in terms of the most relevant descriptors including methyl and hydroxyl anion is expressed by Eq. (2).

$$\begin{aligned} \text{Tumorweight (g)} = & 0.433 + 0.0022(\text{CH}_3/715) + 0.010(\text{CH}_3/838) \\ & - 0.020(\text{CH}_3/465) + 0.0058(\text{HO}^-/833) \\ & + 0.0049(\text{HO}^-/838) \end{aligned} \quad (2)$$

The correlation of the activities tested on the *in vivo* anti-tumor model and calculated using Eq. (2) is explained with Fig. 7. In equation 2 the data points (*n*), correlation coefficient (*r*) and square correlation coefficient (*r*<sup>2</sup>) were 15, 0.987 and 0.975, respectively. The parameters indicated that Eq. (2) is able to predict the *in vivo* activity for **3a–o**.

Eq. (2) contains 3 terms from methyl descriptor and 2 terms from hydroxyl anion descriptor. The terms of 0.0022 (CH<sub>3</sub>/715) and 0.010 (CH<sub>3</sub>/838) have positive coefficients, which means that at these positions small groups will increase the activity, while term of 0.020 (CH<sub>3</sub>/465) has negative coefficient, which means that at this position large group will increase the activity. The terms of 0.0058 (HO<sup>−</sup>/833) and 0.0049 (HO<sup>−</sup>/838) have positive coefficients,

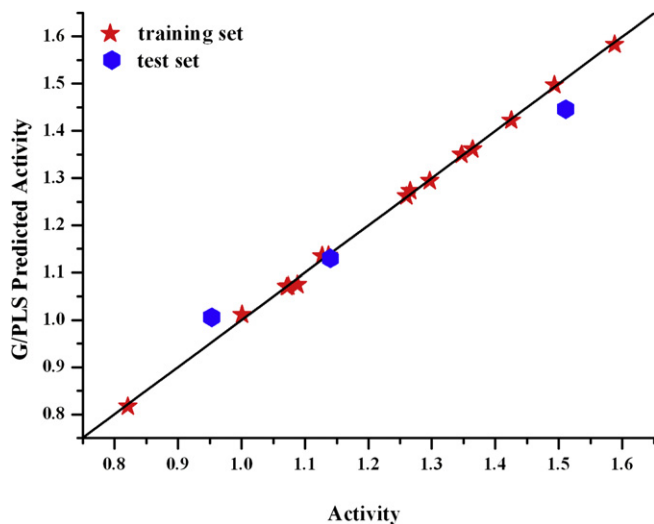


Fig. 7. Graph of tested versus predicted *in vivo* anti-tumor activities of **3a–r**.

Fig. 5 gives **3c, h** as diagrammatic examples of Eq. (1) Compound **3c** has a small group near the region of CH<sub>3</sub>/484 and a hydrogen bond forming group near the region of HO<sup>−</sup>/596, thus it has low *in vitro* anti-proliferation activity. Compound **3h** has small group near the regions of CH<sub>3</sub>/625 and 0.53 CH<sub>3</sub>/944, as well as a large group

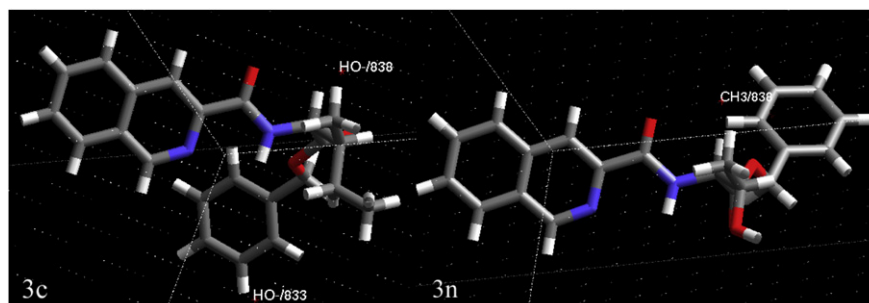


Fig. 8. Electrostatic and environments of **3c** and **3n** within the grid with 3D points of Eq. (2).

**Table 6**  
Apparent permeability coefficients of **2** and **3n, q**.

Compound	$P_{app} \times 10^6 (\text{cm/s})^a$		
	A → B	B → A	A → B/B → A
<b>2</b>	9.47	9.28	1.02
<b>3n</b>	18.61	7.05	2.64
<b>3q</b>	17.22	7.12	2.42

<sup>a</sup> **2** and **3n, q** were dissolved in HBSS (final concentration: 4 mM), the standard deviations were generally less than 9.2% ( $n = 4$ ); A → B: from apical side to basolateral side; B → A: from basolateral side to apical side.

which means that at these positions hydrogen bond forming groups will decrease the activity.

Fig. 8 gives **3c,n** as diagrammatic examples of equation 2. Compound **3c** has hydrogen bond forming groups near the regions of HO<sup>-</sup>/833 and HO<sup>-</sup>/838 and therefore possesses low *in vivo* anti-tumor activity. Compound **3n** has a small group near the region of CH<sub>3</sub>/838 and therefore possesses high *in vivo* anti-tumor activity.

**2.6.2.4. Predicting *in vivo* anti-tumor activity of 3p–r with Eq. (2).** The predict power of Eq. (2) was demonstrated by comparing the calculated and the tested *in vivo* anti-tumor activities of **3p–r** (Table 5). The correlation of the predict value and the test value is also shown in Fig. 7. The results indicate that Eq. (2) rationally gives the *in vivo* anti-tumor activity for **3p–r** and the errors range from –0.01 to 0.053 g. The calculated activity is so approximate to the experimental activity means that Eq. (2) is practical to accurately predict the *in vitro* anti-tumor activity of isoquinoline-3-carbonyl-L-amino acid benzylesters.

#### 2.7. *In vitro* membrane permeation tests of **2** and **3n, q**

To know the contribution of this modification to the enhancement of the permeability the membrane permeability of isoquinoline-3-carboxylic acid and the most potent isoquinoline-3-carbonyl-L-threonine benzylester (**3n**) and isoquinoline-3-carbonyl-L-leucine benzylester (**3q**) were measured on Caco-2 cell monolayers, and the data are summarized in Table 6. The data indicate that modifying isoquinoline-3-carboxylic acid with L-Thr-OBzl and L-Leu-OBzl results in a significant increase of the permeability. Though the bioavailability of a drug is influenced by a series of factors including dissolution, absorption, pre-systemic and systemic metabolism, and elimination, the intestinal mucosa is a significant barrier to ip delivery of drugs into the systemic circulation. Caco-2 cells possess many structural and functional similarities to human enterocytes. After converting isoquinoline-3-carboxylic acid into its deceptive analogue **3n, q** the permeability gains 2.5-fold increases.

### 3. Conclusion

In conclusion, based on the fact that the *in vitro* anti-tumoral activity of isoquinoline-3-carboxylic acid is at least 80-fold higher than that of β-carboline-3-carboxylic acid it is national that isoquinoline-3-carboxylic acid is a desirable lead compound. The modification of isoquinoline-3-carboxylic acid with L-amino acid benzylesters resulted in a class of novel isoquinoline-3-carbonylamino acid benzylesters. The modification resulted in 2.5-fold increases of the membrane permeability, 2.6-fold to 21.3-fold increases of the *in vitro* anti-proliferation activity and 1.0-fold to 4.7-fold increases of the *in vivo* anti-tumor activity. In addition, on S180 mouse model even if the oral dose was lowered to 1 μmol/kg **3g, n, q** still effectively inhibited the tumor growth of the treated S180 mice. The preliminary fluorescence study (see Supporting

Information) defines a concentration-dependent decrease of fluorescence intensities (fluorescence quenching) of **3n** suggests that the action mechanism should be DNA intercalation and ensures that **3a–r** should be DNA intercalators [49]. According to this comment the topoisomerase I induced cleavage of dimeric pRR322 DNA assays were performed for compounds **2** and **3n, o, q**, the results were described with the electrophoresis of the reaction mixtures were analyzed using a 0.8% agarose gel in TRE buffer (Fig. 2 of Supporting Information). The electrophoresis indicates that compounds **2** and **3n, o, q** are the inhibitors of topoisomerase I.

## 4. Experimental section

### 4.1. General method

All the reactions were carried out under nitrogen (1 bar). <sup>1</sup>H (300 and 500 MHz) and <sup>13</sup>C (75 and 125 MHz) NMR spectra were recorded on Bruker AMX-300 and AMX-500 spectrometers for solution DMSO-*d*<sub>6</sub>, or CDCl<sub>3</sub> with tetramethylsilane as internal standard. IR spectra were recorded with a Perkin–Elmer 983 instrument. FAB/MS was determined on VG-ZAB-MS, and TOF-MS was recorded on MDS SCIEX QSTAR. Melting points were measured on a XT5 hot stage microscope (Beijing key electro-optic factory). All L-amino acids were purchased from China Biochemical Corp. TLC was made with Qingdao silica gel GF<sub>254</sub>. Chromatography was performed with Qingdao silica gel H<sub>60</sub> or Sephadex-LH<sub>20</sub>. The purities of the intermediates were measured on TLC (Merck silica gel plates of type 60 F<sub>254</sub>, 0.25 mm layer thickness, three systems of mixed solvents) and gave a point of single component, while the purities of the products were measured on HPLC (Waters, C<sub>18</sub> column 4.6 × 150 mm, three elution systems of mixed solvents) and more than 96%. All solvents were distilled and dried before use according to literature procedures. Optical rotations were determined with a Jasco P-1020 Polarimeter at 20 °C. The statistical analysis of all the biological data was carried out by use of ANOVA test,  $p < 0.05$  is considered significant.

### 4.2. Preparing compounds

#### 4.2.1. (3S)-1,2,3,4-Tetrahydroisoquinoline-3-carboxylic acid (**1**)

To the suspension of 5.0 g (0.03 mmol) of L-Phe in 50 ml of chloroform and 27 ml of formaldehyde 45 ml of concentrated hydrochloric acid was added drop-wise. The reaction mixture was stirred at 80–90 °C for 10 h, and TLC (CHCl<sub>3</sub>/CH<sub>3</sub>OH, 10:1) indicates the complete disappearance of L-Phe. The reaction mixture was cooled to room temperature and the formed precipitates were collected by filtration. The collected solids were successively washed with water (30 ml × 3) and acetone (30 ml × 3) to give 4.5 g (83.9%) of the title compound as a colorless powder. Mp 302–303 °C;  $[\alpha]_D^{20} = -68$  ( $c = 1.0$ , H<sub>2</sub>O); ESI-MS ( $m/e$ ) 178 [M + H]<sup>+</sup>; <sup>1</sup>H NMR (300 MHz, CDCl<sub>3</sub>) δ/ppm = 11.0 (s, 1H), 7.25 (m,  $J = 6.4$  Hz, 2H), 7.02 (d,  $J = 6.5$  Hz, 1H), 6.98 (t,  $J = 6.6$  Hz, 1H), 3.80 (m, 3H), 3.03 (d,  $J = 7.5$  Hz, 1H), 2.78 (d,  $J = 8.4$  Hz, 1H), 2.0 (s, 1H); <sup>13</sup>C NMR (75 MHz, CDCl<sub>3</sub>) δ/ppm = 174.9, 136.2, 134.2, 127.2, 126.0, 57.6, 47.4, 29.4.

#### 4.2.2. Isoquinoline-3-carboxylic acid (**2**)

At 0 °C to a solution of 10.0 g (0.046 mmol) of (3S)-1,2,3,4-tetrahydroisoquinoline-3-carboxylic acid in 200 ml of *N,N*-dimethylformamide 5.0 g (0.032 mmol) of KMnO<sub>4</sub> was added, which took 30 min. The reaction mixture was stirred at room temperature for 100 h, and TLC (CCl<sub>3</sub>:CH<sub>3</sub>OH = 5:1) indicated the complete disappearance of (3S)-1,2,3,4-tetrahydroisoquinoline-3-carboxylic acid. The reaction mixture was evaporated under vacuum. The residue was washed with distilled water repeatedly to provide 8.1 g (83%) of the title compound as a yellow powder. ESI-MS ( $m/e$ ) 174

$[M + H]^+$ ;  $^1H$  NMR (300 MHz, DMSO)  $\delta$ /ppm = 10.81 (s, 1 H), 9.52 (s, 1 H), 8.43 (s, 1 H), 7.52 (m, 4 H);  $^{13}C$  NMR (75 MHz, DMSO)  $\delta$ /ppm = 164.9, 152.3, 143.5, 136.2, 131.3, 129.7, 127.2, 125.8.

#### 4.3. General procedure for preparing **3a–r**

At 0 °C and with stirring to the solution of 865 mg (5.0 mmol) of isoquinoline-3-carboxylic acid in 10 ml of anhydrous THF 675 mg (5.0 mmol) of HOBt was added to form reaction mixture A. The solution of 5.5 mmol of *l*-amino acid benzylester in 5 ml of anhydrous THF was adjusted pH 9 with triethylamine and stirred for 30 min to form mixture B. At 0 °C the mixtures A and B were mixed and then 1339 mg (6.5 mmol) of DCC was added. The reaction mixture was stirred at 0 °C for 2 h, at room temperature for 12 h and TLC (ethyl acetate/petroleum ether, 1:2) indicated the complete disappearance of isoquinoline-3-carboxylic acid. The formed precipitates of DCU were removed by filtration and the filtrate was evaporated under vacuum. The residue was dissolved in 50 ml of ethyl acetate and the formed solution was washed successively with saturated aqueous solution of  $NaHCO_3$  (30 ml  $\times$  3), 5% aqueous solution of  $KHSO_4$  (30 ml  $\times$  3) and saturated aqueous solution of  $NaCl$  (30 ml  $\times$  3) and dried over anhydrous  $Na_2SO_4$ . After filtration the filtrate was evaporated under vacuum and the residue was purified on silica gel chromatography ( $CHCl_3$ :MeOH, 20:1) to give the title compounds.

##### 4.3.1. Benzyl (S)-2-methyl-2-(isoquinoline-3-carboxamido)acetate (**3a**)

Yield: 87%. Colorless powders. ESI-MS (*m/e*) 335  $[M + H]^+$ ;  $[\alpha]_{20}^D = -6.6$  ( $c = 1.0$ ,  $CH_3OH$ ); IR (KBr): 3312, 2972, 2960, 2883, 2870, 1710, 1690, 1450, 1380  $cm^{-1}$ ;  $^1H$  NMR (300 MHz, DMSO)  $\delta$ /ppm = 9.41 (s, 1 H), 9.16 (s, 1 H), 8.59 (s, 1 H), 8.24 (q,  $J = 8.4$  Hz, 2 H), 7.85 (m, 2 H), 7.35 (m, 5 H), 5.18 (s, 2 H), 4.70 (m, 1 H), 1.51 (d,  $J = 8.6$  Hz, 3 H);  $^{13}C$  NMR (75 MHz, DMSO)  $\delta$ /ppm = 172.7, 164.9, 152.8, 151.0, 142.9, 138.2, 131.6, 129.6, 129.1, 127.6, 127.3, 124.8, 66.7, 48.6, 17.6. Anal. Calcd for  $C_{20}H_{18}N_2O_3$ : C, 71.84; H, 5.43; N, 8.38. Found C, 71.67; H, 5.54; N, 8.15.

##### 4.3.2. Benzyl (S)-2-(2-propyl)-2-(isoquinoline-3-carboxamido)acetate (**3b**)

Yield: 87%. Colorless powders. ESI-MS (*m/e*) 363  $[M + H]^+$ ;  $[\alpha]_{20}^D = -4.9$  ( $c = 1.0$ ,  $CH_3OH$ ); IR (KBr): 3312, 2972, 2961, 2890, 2869, 1710, 1690, 1385, 1375, 599  $cm^{-1}$ ;  $^1H$  NMR (300 MHz, DMSO)  $\delta$ /ppm = 9.42 (s, 1 H), 8.60 (s, 1 H), 8.24 (q,  $J = 8.4$  Hz, 2 H), 7.86 (m, 2 H), 7.36 (m, 5 H), 5.21 (q,  $J = 8.4$  Hz, 2 H), 4.57 (t,  $J = 8.5$  Hz, 1 H), 2.30 (m, 1 H), 0.95 (d,  $J = 8.6$  Hz, 6 H);  $^{13}C$  NMR (75 MHz, DMSO)  $\delta$ /ppm = 171.6, 164.5, 152.3, 151.3, 143.0, 136.0, 132.1, 128.6, 124.5, 66.7, 57.0, 30.8, 25.4, 19.0. Anal. Calcd for  $C_{22}H_{22}N_2O_3$ : C, 72.91; H, 6.12; N, 7.73. Found C, 72.70; H, 6.25; N, 7.50.

##### 4.3.3. Benzyl (S)-2-(2-butyl)-2-(isoquinoline-3-carboxamido)acetate (**3c**)

Yield: 75%. Colorless powders. ESI-MS (*m/e*) 377  $[M + H]^+$ ;  $[\alpha]_{20}^D = -4.2$  ( $c = 1.0$ ,  $CH_3OH$ ); IR (KBr): 3312, 2972, 2960, 2890, 2871, 1710, 1690, 1450, 1380, 600  $cm^{-1}$ ;  $^1H$  NMR (300 MHz, DMSO)  $\delta$ /ppm = 9.42 (s, 1 H), 8.80 (d, 1 H), 8.59 (s, 1 H), 8.24 (q,  $J = 8.4$  Hz, 2 H), 7.86 (m, 2 H), 7.36 (m, 5 H), 5.21 (s, 2 H), 4.62 (t,  $J = 8.5$  Hz, 1 H), 2.51 (m, 1 H), 1.30 (m, 2 H), 0.96 (m, 6 H);  $^{13}C$  NMR (75 MHz, DMSO)  $\delta$ /ppm = 171.6, 164.4, 152.3, 143.3, 136.0, 132.1, 131.2, 129.5, 128.6, 127.6, 127.2, 120.5, 66.7, 57.0, 37.2, 25.4, 16.0, 11.6; Anal. Calcd for  $C_{23}H_{24}N_2O_3$ : C, 73.38; H, 6.43; N, 7.44. Found C, 73.15; H, 6.57; N, 7.22.

##### 4.3.4. Benzyl (S)-2-(1H-indol-3-ylmethyl)-2-(isoquinoline-3-carboxamido)acetate (**3d**)

Yield: 59%. Colorless powders. ESI-MS (*m/e*) 450  $[M + H]^+$ ;  $[\alpha]_{20}^D = -3.1$  ( $c = 1.0$ ,  $CH_3OH$ ); IR (KBr): 3410, 3312, 2972, 2883,

1379, 1087, 1050, 881, 800, 620  $cm^{-1}$ ;  $^1H$  NMR (300 MHz, DMSO)  $\delta$ /ppm = 10.11 (s, 1 H), 9.44 (s, 1 H), 8.58 (s, 1 H), 8.24 (q,  $J = 8.4$  Hz, 2 H), 8.01 (d,  $J = 8.6$  Hz, 1 H), 7.86 (m, 2 H), 7.19 (m, 9 H), 6.85 (d,  $J = 8.6$  Hz, 1 H), 5.34 (s, 2 H), 4.81 (q,  $J = 8.4$  Hz, 1 H), 3.02 (m, 2 H);  $^{13}C$  NMR (75 MHz, DMSO)  $\delta$ /ppm = 171.9, 165.1, 152.1, 150.8, 143.6, 138.6, 132.1, 131.2, 129.6, 129.0, 128.5, 124.8, 122.8, 122.3, 120.1, 119.2, 111.3, 110.5, 68.7, 58.0, 28.9; Anal. Calcd for  $C_{28}H_{23}N_3O_3$ : C, 74.82; H, 5.16; N, 9.35. Found C, 74.60; H, 5.31; N, 9.12.

##### 4.3.5. Benzyl (S)-2-hydroxymethyl-2-(isoquinoline-3-carboxamido)acetate (**3e**)

Yield: 84%. Colorless powders. ESI-MS (*m/e*) 441  $[M + H]^+$ ;  $[\alpha]_{20}^D = -7.1$  ( $c = 1.0$ ,  $CH_3OH$ ); IR (KBr): 3413, 2969, 1734, 1648, 1497, 1457, 1440, 1198, 1111  $cm^{-1}$ ;  $^1H$  NMR (300 MHz, DMSO)  $\delta$ /ppm = 9.44 (s, 1 H), 8.75 (d,  $J = 8.6$  Hz, 1 H), 8.58 (s, 1 H), 8.24 (q,  $J = 8.4$  Hz, 2 H), 7.86 (m, 2 H), 7.32 (m, 10 H), 5.32 (s, 2 H), 4.74 (m, 1 H), 4.61 (s, 2 H), 4.01 (m, 2 H);  $^{13}C$  NMR (75 MHz, DMSO)  $\delta$ /ppm = 170.6, 164.6, 152.2, 143.4, 139.0, 137.6, 132.1, 129.6, 128.5, 127.2, 124.8, 79.2, 72.4, 66.7, 53.0; Anal. Calcd for  $C_{27}H_{24}N_2O_4$ : C, 73.62; H, 5.49; N, 6.36. Found C, 73.40; H, 5.62; N, 6.11.

##### 4.3.6. Benzyl (S)-2-(4-hydroxybenzyl)-2-(isoquinoline-3-carboxamido)acetate (**3f**)

Yield: 56%. Colorless powders. ESI-MS (*m/e*) 427  $[M + H]^+$ ;  $[\alpha]_{20}^D = -3.2$  ( $c = 1.0$ ,  $CH_3OH$ ); IR (KBr): 3420, 2969, 1734, 1648, 1600, 1497, 1450, 1440, 1198, 1110  $cm^{-1}$ ;  $^1H$  NMR (300 MHz, DMSO)  $\delta$ /ppm = 9.44 (s, 1 H), 8.75 (d,  $J = 8.6$  Hz, 1 H), 8.58 (s, 1 H), 8.24 (q,  $J = 8.4$  Hz, 2 H), 7.86 (m, 2 H), 7.22 (m, 5 H), 6.96 (d,  $J = 8.8$  Hz, 2 H), 6.69 (d,  $J = 8.8$  Hz, 2 H), 5.17 (s, 2 H), 4.74 (m, 1 H), 3.31 (dd,  $J = 3.6$  Hz, 12.1 Hz, 1 H), 3.05 (dd,  $J = 3.6$  Hz, 12.1 Hz, 1 H);  $^{13}C$  NMR (75 MHz, DMSO)  $\delta$ /ppm = 170.6, 164.6, 155.6, 152.2, 151.7, 143.4, 137.6, 132.1, 131.5, 128.5, 124.8, 79.2, 72.4, 66.7, 57.0, 16.7; Anal. Calcd for  $C_{26}H_{22}N_2O_4$ : C, 73.23; H, 5.20; N, 6.57. Found C, 73.00; H, 5.34; N, 6.23.

##### 4.3.7. Benzyl (S)-2-(1-isoquinoline-3-carbonylpyrrolidine-2-yl)acetate (**3g**)

Yield: 76%. Colorless powders. ESI-MS (*m/e*) 361  $[M + H]^+$ ;  $[\alpha]_{20}^D = -2.0$  ( $c = 1.0$ ,  $CH_3OH$ ); IR (KBr): 3411, 2969, 1734, 1650, 1497, 1457, 1375, 1198, 1111, 750, 599  $cm^{-1}$ ;  $^1H$  NMR (300 MHz, DMSO)  $\delta$ /ppm = 9.44 (s, 1 H), 8.58 (s, 1 H), 8.24 (q,  $J = 8.4$  Hz, 2 H), 7.86 (m, 2 H), 7.32 (m, 5 H), 5.34 (s, 2 H), 4.18 (t,  $J = 8.5$  Hz, 1 H), 3.35 (t,  $J = 8.5$  Hz, 2 H), 1.96 (q,  $J = 8.4$  Hz, 2 H), 1.60 (m, 2 H);  $^{13}C$  NMR (75 MHz, DMSO)  $\delta$ /ppm = 171.9, 165.1, 152.1, 150.8, 143.6, 138.6, 132.1, 129.6, 129.1, 128.5, 127.6, 124.8, 68.7, 58.0, 46.1, 28.9, 22.1; Anal. Calcd for  $C_{22}H_{20}N_2O_3$ : C, 73.32; H, 5.59; N, 7.77. Found C, 73.11; H, 5.75; N, 7.54.

##### 4.3.8. Benzyl (S)-2-(2-aminocarbonyl-ethyl-1-yl)-2-(isoquinoline-3-carboxamido)acetate (**3h**)

Yield: 53%. Colorless powders. ESI-MS (*m/e*) 392  $[M + H]^+$ ;  $[\alpha]_{20}^D = 3.33$  ( $c = 1.0$ ,  $CH_3OH$ ); IR (KBr): 3414, 2970, 1734, 1648, 1498, 1457, 1375, 1198, 750, 599  $cm^{-1}$ ;  $^1H$  NMR (300 MHz, DMSO)  $\delta$ /ppm = 9.44 (s, 1 H), 8.75 (d,  $J = 8.6$  Hz, 1 H), 8.58 (s, 1 H), 8.24 (q,  $J = 8.4$  Hz, 2 H), 7.86 (m, 2 H), 7.32 (m, 5 H), 6.0 (s, 2 H), 5.34 (s, 2 H), 4.45 (q,  $J = 8.4$  Hz, 1 H), 2.98 (q,  $J = 8.4$  Hz, 2 H), 2.16 (q,  $J = 8.4$  Hz, 2 H);  $^{13}C$  NMR (75 MHz, DMSO)  $\delta$ /ppm = 172.6, 171.8, 165.0, 152.1, 150.8, 143.6, 138.6, 132.1, 128.5, 127.6, 127.2, 124.8, 68.7, 52.0, 33.1, 28.3; Anal. Calcd for  $C_{22}H_{21}N_3O_4$ : C, 67.51; H, 5.41; N, 10.74. Found C, 67.31; H, 5.55; N, 10.51.

##### 4.3.9. Benzyl (S)-2-(imidazol-4-ylmethyl)-2-(isoquinoline-3-carboxamido)acetate (**3i**)

Yield: 55%. Colorless powders. ESI-MS (*m/e*) 401  $[M + H]^+$ ;  $[\alpha]_{20}^D = -4.7$  ( $c = 1.0$ ,  $CH_3OH$ ); IR (KBr): 3420, 2969, 1734, 1648,

1497, 1457, 1375, 1198, 1200, 750  $\text{cm}^{-1}$ ;  $^1\text{H}$  NMR (300 MHz, DMSO)  $\delta/\text{ppm}$  = 13.12 (s, 1 H), 9.44 (s, 1 H), 8.58 (s, 1 H), 8.24 (q,  $J$  = 8.4 Hz, 2 H), 8.02 (d,  $J$  = 8.6 Hz, 1 H), 7.86 (m, 2 H), 7.44 (s, 1 H), 7.19 (m, 5 H), 6.82 (d,  $J$  = 8.6 Hz, 1 H), 5.34 (s, 2 H), 4.81 (q,  $J$  = 8.4 Hz, 1 H), 3.12 (m, 2 H);  $^{13}\text{C}$  NMR (75 MHz, DMSO)  $\delta/\text{ppm}$  = 171.9, 165.1, 152.1, 150.8, 143.6, 138.6, 135.8, 132.1, 129.6, 129.1, 128.5, 127.2, 124.8, 110.5, 68.7, 58.0, 28.9; Anal. Calcd for  $\text{C}_{23}\text{H}_{20}\text{N}_4\text{O}_3$ : C, 68.99; H, 5.03; N, 13.99. Found C, 68.76; H, 5.18; N, 13.73.

#### 4.3.10. Benzyl (S)-2-(4-aminobutyl-1-yl)-2-(isoquinoline-3-carboxamido)acetate (**3j**)

Yield: 90%. Colorless powders. ESI-MS ( $m/e$ ) 392  $[\text{M} + \text{H}]^+$ ;  $[\alpha]_{20}^{\text{D}}$  = 3.6 ( $c$  = 1.0,  $\text{CH}_3\text{OH}$ ); IR (KBr): 3411, 2969, 1735, 1651, 1496, 1458, 1376, 1198, 725, 600  $\text{cm}^{-1}$ ;  $^1\text{H}$  NMR (300 MHz, DMSO)  $\delta/\text{ppm}$  = 9.44 (s, 1 H), 8.58 (s, 1 H), 8.24 (d,  $J$  = 8.6 Hz, 2 H), 8.01 (d,  $J$  = 8.6 Hz, 1 H), 7.86 (m, 2 H), 7.19 (m, 5 H), 5.34 (s, 2 H), 4.41 (q,  $J$  = 8.4 Hz, 1 H), 2.62 (m, 2 H), 2.01 (t,  $J$  = 8.5 Hz, 2 H), 1.90 (q,  $J$  = 8.4 Hz, 2 H), 1.55 (m, 2 H), 1.29 (m, 2 H);  $^{13}\text{C}$  NMR (75 MHz, DMSO)  $\delta/\text{ppm}$  = 171.9, 165.1, 152.1, 150.8, 143.6, 138.6, 132.1, 129.6, 128.5, 127.2, 127.0, 124.8, 110.5, 68.7, 53.0, 42.3, 32.5, 31.1, 21.1; Anal. Calcd for  $\text{C}_{23}\text{H}_{25}\text{N}_3\text{O}_3$ : C, 70.57; H, 6.44; N, 10.73. Found C, 70.34; H, 6.61; N, 10.50.

#### 4.3.11. Benzyl (S)-2-benzoyloxycarbonylmethyl-2-(isoquinoline-3-carboxamido)acetate (**3k**)

Yield: 77%. Colorless powders. ESI-MS ( $m/e$ ) 483  $[\text{M} + \text{H}]^+$ ;  $[\alpha]_{20}^{\text{D}}$  = 22.1 ( $c$  = 1.0,  $\text{CH}_3\text{OH}$ ); IR (KBr): 3411, 2969, 1734, 1648, 1497, 1457, 1390, 1198, 750, 599  $\text{cm}^{-1}$ ;  $^1\text{H}$  NMR (300 MHz, DMSO)  $\delta/\text{ppm}$  = 9.44 (s, 1 H), 8.75 (d,  $J$  = 8.6 Hz, 1 H), 8.58 (s, 1 H), 8.24 (q,  $J$  = 8.4 Hz, 2 H), 7.86 (m, 2 H), 7.32 (m, 10 H), 5.17 (m, 4 H), 4.45 (q,  $J$  = 8.4 Hz, 1 H), 2.51 (m, 4 H);  $^{13}\text{C}$  NMR (75 MHz, DMSO)  $\delta/\text{ppm}$  = 172.6, 171.8, 165.0, 152.1, 143.6, 138.6, 132.1, 129.5, 128.5, 127.4, 126.9, 124.8, 79.2, 72.4, 68.7, 52.0, 28.1, 26.7; Anal. Calcd for  $\text{C}_{29}\text{H}_{26}\text{N}_2\text{O}_5$ : C, 72.18; H, 5.43; N, 5.81. Found C, 72.00; H, 5.55; N, 5.60.

#### 4.3.12. Benzyl (S)-2-(2-benzoyloxycarbonyl-ethyl-1-yl)-2-(isoquinoline-3-carboxamido)acetate (**3l**)

Yield: 83%. Colorless powders. ESI-MS ( $m/e$ ) 469  $[\text{M} + \text{H}]^+$ ;  $[\alpha]_{20}^{\text{D}}$  = 13.1 ( $c$  = 1.0,  $\text{CH}_3\text{OH}$ ); IR (KBr): 3413, 2969, 1734, 1648, 1497, 1457, 1375, 1198, 1111, 750, 599  $\text{cm}^{-1}$ ;  $^1\text{H}$  NMR (300 MHz, DMSO)  $\delta/\text{ppm}$  = 9.44 (s, 1 H), 8.75 (d,  $J$  = 8.6 Hz, 1 H), 8.58 (s, 1 H), 8.24 (q,  $J$  = 8.4 Hz, 2 H), 7.86 (m, 2 H), 7.32 (m, 10 H), 5.17 (m, 4 H), 4.75 (q,  $J$  = 8.4 Hz, 1 H), 2.51 (m, 2 H);  $^{13}\text{C}$  NMR (75 MHz, DMSO)  $\delta/\text{ppm}$  = 172.6, 171.8, 165.0, 152.1, 143.6, 138.6, 132.1, 129.4, 128.5, 127.3, 127.0, 124.8, 79.2, 72.4, 66.7, 47.0, 36.7; Anal. Calcd for  $\text{C}_{28}\text{H}_{24}\text{N}_2\text{O}_5$ : C, 71.78; H, 5.16; N, 5.98. Found C, 71.56; H, 5.31; N, 5.74.

#### 4.3.13. Benzyl (S)-2-benzyl-2-(isoquinoline-3-carboxamido)acetate (**3m**)

Yield: 87%. Colorless powders. ESI-MS ( $m/e$ ) 411  $[\text{M} + \text{H}]^+$ ;  $[\alpha]_{20}^{\text{D}}$  = -3.1 ( $c$  = 1.0,  $\text{CH}_3\text{OH}$ ); IR (KBr): 3312, 2972, 2883, 1600, 1500, 1450, 1379, 1087, 1050, 881, 620  $\text{cm}^{-1}$ ;  $^1\text{H}$  NMR (300 MHz, DMSO)  $\delta/\text{ppm}$  = 9.39 (s, 1 H), 9.08 (d,  $J$  = 8.6 Hz, 1 H), 8.54 (s, 1 H), 8.24 (q,  $J$  = 8.4 Hz, 2 H), 7.86 (m, 2 H), 7.26 (m, 10 H), 5.18 (s, 2 H), 4.94 (q,  $J$  = 8.4 Hz, 1 H), 3.32 (m, 2 H);  $^{13}\text{C}$  NMR (75 MHz, DMSO)  $\delta/\text{ppm}$  = 171.6, 164.6, 152.2, 143.4, 137.6, 132.1, 129.1, 128.5, 127.3, 127.1, 124.8, 66.7, 57.0, 36.8; Anal. Calcd for  $\text{C}_{26}\text{H}_{22}\text{N}_2\text{O}_3$ : C, 76.08; H, 5.40; N, 6.82. Found C, 75.85; H, 5.56; N, 6.59.

#### 4.3.14. Benzyl (S)-2-(1-hydroxyethyl-1-yl)-2-(isoquinoline-3-carboxamido)acetate (**3n**)

Yield: 77%. Colorless powders. ESI-MS ( $m/e$ ) 455  $[\text{M} + \text{H}]^+$ ;  $[\alpha]_{20}^{\text{D}}$  = -3.2 ( $c$  = 1.0,  $\text{CH}_3\text{OH}$ ); IR (KBr): 3410, 2969, 1734, 1648, 1497, 1457, 1440, 1380, 1198, 1112  $\text{cm}^{-1}$ ;  $^1\text{H}$  NMR (300 MHz, DMSO)  $\delta/\text{ppm}$  = 9.44 (s, 1 H), 8.75 (d,  $J$  = 8.6 Hz, 1 H), 8.58 (s, 1 H), 8.24 (q,

$J$  = 8.4 Hz, 2 H), 7.86 (m, 2 H), 7.32 (m, 10 H), 5.17 (s, 2 H), 4.74 (m, 1 H), 4.61 (s, 2 H), 4.27 (m, 1 H), 1.26 (d,  $J$  = 8.6 Hz, 3 H);  $^{13}\text{C}$  NMR (75 MHz, DMSO)  $\delta/\text{ppm}$  = 170.6, 164.6, 152.2, 150.8, 143.4, 137.6, 132.1, 131.0, 129.5, 128.5, 127.9, 127.2, 124.8, 79.2, 72.4, 66.7, 57.0, 16.7; Anal. Calcd for  $\text{C}_{28}\text{H}_{26}\text{N}_2\text{O}_4$ : C, 73.99; H, 5.77; N, 6.16. Found C, 73.76; H, 5.94; N, 5.93.

#### 4.3.15. Benzyl (S)-2-(2-methylmercaptoethyl-1-yl)-2-(isoquinoline-3-carboxamido)acetate (**3o**)

Yield: 83%. Colorless powders. ESI-MS ( $m/e$ ) 395  $[\text{M} + \text{H}]^+$ ;  $[\alpha]_{20}^{\text{D}}$  = -1.3 ( $c$  = 1.0,  $\text{CH}_3\text{OH}$ ); IR (KBr): 3410, 2969, 1734, 1648, 1497, 1457, 1380, 1198, 1113, 750  $\text{cm}^{-1}$ ;  $^1\text{H}$  NMR (300 MHz, DMSO)  $\delta/\text{ppm}$  = 9.44 (s, 1 H), 8.75 (d,  $J$  = 8.6 Hz, 1 H), 8.58 (s, 1 H), 8.24 (q,  $J$  = 8.4 Hz, 2 H), 7.86 (m, 2 H), 7.32 (m, 5 H), 5.34 (s, 2 H), 4.45 (q,  $J$  = 8.4 Hz, 1 H), 2.48 (t,  $J$  = 8.5 Hz, 2 H), 2.26 (q,  $J$  = 8.4 Hz, 2 H), 2.10 (s, 3 H);  $^{13}\text{C}$  NMR (75 MHz, DMSO)  $\delta/\text{ppm}$  = 171.9, 165.1, 152.1, 150.8, 143.6, 138.6, 132.1, 129.6, 129.0, 128.5, 127.7, 127.1, 124.8, 68.7, 52.0, 31.1, 30.3, 15.0; Anal. Calcd for  $\text{C}_{22}\text{H}_{22}\text{N}_2\text{O}_3\text{S}$ : C, 66.98; H, 5.62; N, 7.10. Found C, 66.77; H, 5.75; N, 6.88.

#### 4.3.16. Benzyl 2-(isoquinoline-3-carboxamido)acetate (**3p**)

Yield: 79%. Colorless powders. ESI-MS ( $m/e$ ) 321  $[\text{M} + \text{H}]^+$ ;  $[\alpha]_{20}^{\text{D}}$  = 5.6 ( $c$  = 1.0,  $\text{CH}_3\text{OH}$ ); IR (KBr): 3312, 2972, 2961, 2883, 2869, 1710, 1690, 1440  $\text{cm}^{-1}$ ;  $^1\text{H}$  NMR (300 MHz, DMSO)  $\delta/\text{ppm}$  = 9.44 (s, 1 H), 8.68 (s, 1 H), 8.24 (q,  $J$  = 8.4 Hz, 2 H), 7.87 (m, 2 H), 7.43 (m, 5 H), 7.31 (s, 1 H), 5.44 (s, 2 H), 4.41 (d,  $J$  = 8.6 Hz, 2 H);  $^{13}\text{C}$  NMR (75 MHz, DMSO)  $\delta/\text{ppm}$  = 169.7, 161.9, 151.8, 151.0, 141.9, 137.2, 130.6, 129.5, 129.1, 127.2, 124.9, 67.7, 41.6. Anal. Calcd for  $\text{C}_{19}\text{H}_{16}\text{N}_2\text{O}_3$ : C, 71.24; H, 5.03; N, 8.74. Found C, 71.05; H, 5.17; N, 8.51.

#### 4.3.17. Benzyl (S)-2-(2-methylpropyl-1-yl)-2-(isoquinoline-3-carboxamido)acetate (**3q**)

Yield: 81%. Colorless powders. ESI-MS ( $m/e$ ) 377  $[\text{M} + \text{H}]^+$ ;  $[\alpha]_{20}^{\text{D}}$  = -5.1 ( $c$  = 1.0,  $\text{CH}_3\text{OH}$ ); IR (KBr): 3312, 2972, 2961, 2890, 2869, 1710, 1690, 1385, 1375, 599  $\text{cm}^{-1}$ ;  $^1\text{H}$  NMR (300 MHz, DMSO)  $\delta/\text{ppm}$  = 8.54 (s, 1 H), 8.08 (s, 1 H), 8.24 (q,  $J$  = 8.4 Hz, 2 H), 7.87 (m, 2 H), 7.36 (m, 5 H), 7.31 (s, 1 H), 5.15 (s, 2 H), 4.42 (t,  $J$  = 8.5 Hz, 1 H), 1.58 (m, 3 H), 0.86 (d,  $J$  = 8.6 Hz, 6 H);  $^{13}\text{C}$  NMR (75 MHz, DMSO)  $\delta/\text{ppm}$  = 172.4, 161.5, 152.8, 151.1, 142.9, 136.4, 128.6, 131.5, 129.6, 129.0, 127.6, 127.0, 124.9, 68.5, 48.7, 40.7, 23.8, 22.8; Anal. Calcd for  $\text{C}_{23}\text{H}_{24}\text{N}_2\text{O}_3$ : C, 73.38; H, 6.43; N, 7.44. Found C, 73.16; H, 6.57; N, 7.20.

#### 4.3.18. Benzyl (S)-2-aminocarbonylmethyl-2-(isoquinoline-3-carboxamido)acetate (**3r**)

Yield: 54%. Colorless powders. ESI-MS ( $m/e$ ) 378  $[\text{M} + \text{H}]^+$ ;  $[\alpha]_{20}^{\text{D}}$  = 6.3 ( $c$  = 1.0,  $\text{CH}_3\text{OH}$ ); IR (KBr): 3415, 2969, 1734, 1648, 1497, 1457, 1375, 1198, 750, 599  $\text{cm}^{-1}$ ;  $^1\text{H}$  NMR (300 MHz, DMSO)  $\delta/\text{ppm}$  = 9.44 (s, 1 H), 8.75 (d,  $J$  = 8.6 Hz, 1 H), 8.58 (s, 1 H), 8.24 (q,  $J$  = 8.4 Hz, 2 H), 7.86 (m, 2 H), 7.32 (m, 5 H), 6.0 (s, 2 H), 5.34 (s, 2 H), 4.65 (q,  $J$  = 8.4 Hz, 1 H), 2.78 (m, 2 H);  $^{13}\text{C}$  NMR (75 MHz, DMSO)  $\delta/\text{ppm}$  = 172.6, 171.8, 165.0, 152.1, 150.8, 143.6, 138.6, 132.1, 129.6, 128.5, 127.7, 127.6, 127.1, 124.8, 68.7, 52.0, 38.1; Anal. Calcd for  $\text{C}_{21}\text{H}_{19}\text{N}_3\text{O}_4$ : C, 66.83; H, 5.07; N, 11.13. Found C, 66.62; H, 5.23; N, 10.90.

### 4.4. Bioassay

#### 4.4.1. In vitro anti-proliferation assay

According to the slightly modified procedure of Al-Allaf and Rashan [13], the in vitro anti-proliferation assays were carried out by use of 96 microtiter plate cultures and MTT staining. The HL-60 and Hela cells (obtained from Department of Biochemistry, Capital University of Medical Sciences, final concentration in the growth medium was  $1 \times 10^4/\text{ml}$ ) were grown in RPMI-1640 medium

(containing 10%, v/v) FCS, penicillin (100 µg/ml) and streptomycin (100 µg/ml) without (for control) or with **3a–r** (in a series of final concentrations ranging from 1 mM to 1 nM). The cultures were propagated at 37 °C in a humidified atmosphere containing 5% CO<sub>2</sub> for 24 h, after the first renew of the growth medium without (for control) or with **3a–r** (for test sample) were propagated for another 48 h, after the second renew of the growth medium without (for control) or with **3a–r** (for test sample) were propagated for another 4 h. The growth medium was removed and the residue was dried in the air. The dried residues were dissolved in 100 µl of DMSO and the absorption values of light of the formed purple solutions were recorded on Bio-rad 450 microplate reader (Biorad, USA). The inhibited rates were calculated according to  $I\% = \frac{(C - T)}{C}$ . Wherein C presents the absorption value of light of the control and T presents the absorption value of light of the test sample. The IC<sub>50</sub> values were determined via program GWBASIS.EXE.

#### 4.4.2. In vivo anti-tumor assay

Male ICR mice, purchased from Peking University Health Science Center, were maintained at 21 °C with a natural day/night cycle in a conventional animal colony. The mice were 10–12 weeks old at the beginning of the experiments. The tumor used was S180 which forms solid tumors, when injected subcutaneously. S180 cells for initiation of subcutaneous tumors were obtained from the ascitic form of the tumors in mice, which were serially transplanted once per week. Subcutaneous tumors were implanted by injecting 0.2 ml of NS containing  $1 \times 10^7$  viable tumor cells under the skin on the right oter. Twenty-four hours after implantation, the tumor-bearing mice were randomized into 20 experimental groups (10 per group). All the mice were given a daily i.p. injection of cytarabine (positive control, 100 µmol/kg/day in 0.2 ml of NS), or NS (negative control, 0.2 ml), or **3a–r** (100 µmol/kg/day in 0.2 ml of NS) for 7 consecutive days. Twenty-four hours after the last administration, all mice were sacrificed by diethyl ether anesthesia and the tumors were dissected and weighed. The inhibitory rate of tumor growth was calculated using the equation: Inhibition = (Tumor weight from negative control mice) – (Tumor weight from **3a–r** or cytarabine treated mice) ÷ (Tumor weight from negative control mice).

#### 4.4.3. In vivo dose-dependent assay of oral administration of **3g, n, q**

Male ICR mice, purchased from Peking University Health Science Center, were maintained at 21 °C with a natural day/night cycle in a conventional animal colony. The mice were 10–12 weeks old at the beginning of the experiments. The tumor used was S180 which forms solid tumors, when injected subcutaneously. S180 cells for initiation of subcutaneous tumors were obtained from the ascitic form of the tumors in mice, which were serially transplanted once per week. Subcutaneous tumors were implanted by injecting 0.2 ml of NS containing  $1 \times 10^7$  viable tumor cells under the skin on the right oter. Twenty-four hours after implantation, the tumor-bearing mice were randomized into 20 experimental groups (10 per group). All the mice were given a daily i.p. injection of cytarabine (positive control, 100 µmol/kg/day in 0.2 ml of NS), or a daily oral administration of NS (negative control, 0.2 ml), or **3g, n, q** (100, 10 or 1 µmol/kg/day in 0.2 ml of NS) for 7 consecutive days. Twenty-four hours after the last administration, all mice were sacrificed by diethyl ether anesthesia and the tumors were dissected and weighed. The inhibitory rate of tumor growth was calculated according to the formula of Section 4.4.2.

#### 4.5. Apparent permeability coefficient test of **2** and **3n, q**

Caco-2 cells (from the American Type Culture Collection, Rockville, MD, USA) were cultivated on polycarbonate filters (transwell

cell culture inserts, 12 mm in diameter, 3.0 µm in mean pore size). Caco-2 cells were grown on filter supports and the integrity of monolayers was routinely checked by measurements of trans-epithelial electrical resistance (approximately 700 Ω cm<sup>2</sup>). Compounds **2** and **3n, q** for evaluation were dissolved in HBSS to prepare drug solutions at a final concentration of 4 mM. In apical to basolateral direction, transport was initiated by adding drug solutions (total AP volume, 0.5 ml) to the apical compartment of inserts held in transwells containing 1.5 ml of HBSS (basolateral compartment). In basolateral to apical direction, transport was initiated by adding 1.5 ml of the solution of **2** and **3n, q** to basolateral compartment and adding 0.5 ml of HBSS as receiving solution to apical side of the monolayers. The monolayers were incubated in air at 37 °C and 95% relative humidity. At 30, 60, 90, and 120 min, samples were withdrawn from the receiving side, and the concentrations of the samples were determined by HPLC analysis. The resistance of monolayers was checked at the end of each test. Apparent permeability coefficients (P<sub>app</sub>) were calculated according to  $P_{app} = \frac{dQ}{dt} \cdot \frac{1}{(A \cdot C_0)}$ , wherein  $\frac{dQ}{dt}$  is the permeability rate,  $C_0$  is the initial concentration in the donor chamber, and A is the surface area of monolayer (1 cm<sup>2</sup>).

#### Acknowledgements

This work was completed in the Beijing area major laboratory of peptide and small molecular drugs, supported by PHR (IHLB, KZ 200810025010), the National Natural Scientific Foundation of China (20772082, 30801426, 30901843), and Special Project (2008ZX09401-002) of China.

#### Appendix A. Supplementary information

Supplementary information associated with this article can be found in the online version, at doi:10.1016/j.ejmech.2011.02.017.

#### References

- [1] A.K. Verma, S. Bansal, J. Singh, R.K. Tiwari, V.K. Sankar, V. Tandon, R. Chandra, *Bioorg. Med. Chem.* 14 (2006) 6733–6735.
- [2] R. Aneja, S.N. Vangapandu, H.C. Joshi, *Bioorg. Med. Chem.* 14 (2006) 8352–8358.
- [3] A. Bermejo, I. Andreu, F. Suvire, S. Léonce, D.H. Caignard, P. Renard, A. Pierré, R.D. Enriz, D. Cortes, N. Cabedo, *J. Med. Chem.* 45 (2002) 5058–5068.
- [4] H. Lin, D.J. Abraham, *Bioorg. Med. Chem. Lett.* 16 (2006) 4178–4183.
- [5] C. Chen, Y. Zhu, X. Liu, Z. Lu, Q. Xie, N. Ling, *J. Med. Chem.* 44 (2001) 4001–4010.
- [6] D. Vásquez, J.A. Rodríguez, C. Theoduloz, J. Verrax, P.B. Calderon, J.A. Valderrama, *Bioorg. Med. Chem. Lett.* 19 (2009) 5060–5062.
- [7] J.A. Valderrama, J.A. Ibacache, V. Arancibia, J. Rodriguez, C. Theoduloz, *Bioorg. Med. Chem.* 17 (2009) 2894–2901.
- [8] I. Gomez-Monterrey, P. Campiglia, P. Grieco, M.V. Diurno, A. Bolognese, P.L. Collac, E. Novellino, *Bioorg. Med. Chem.* 11 (2003) 3769–3775.
- [9] A.L. Smith, F.F. DeMorin, N.A. Paras, Q. Huang, J.K. Petkus, E.M. Doherty, T. Nixey, J.L. Kim, D.A. Whittington, L.F. Epstein, M.R. Lee, M.J. Rose, C. Babji, M. Fernando, K. Hess, Q. Le, P. Beltran, J. Carnahan, *J. Med. Chem.* 52 (2009) 6189–6192.
- [10] S.H. Kim, S.M. Oh, J.H. Song, D. Cho, Q.M. Le, S.H. Lee, W.J. Cho, T.S. Kim, *Bioorg. Med. Chem.* 16 (2008) 1125–1132.
- [11] P. Chen, D. Norris, K.D. Haslow, T.G.M. Dhar, W.J. Pitts, S.H. Watterson, D.L. Cheney, D.A. Bassolino, C.A. Fleener, K.A. Rouleau, D.L. Hollenbaugh, R.M. Townsend, J.C. Barrish, E.J. Iwanowicz, *Bioorg. Med. Chem. Lett.* 13 (2003) 1345–1348.
- [12] C.L. Woodard, S.M. Keenan, L. Gerena, W.J. Welsh, J.A. Geyer, N.C. Waters, *Bioorg. Med. Chem. Lett.* 17 (2007) 4961–4966.
- [13] W. Klinkhammer, H. Müller, C. Globisch, I.K. Pajeva, M. Wiese, *Bioorg. Med. Chem.* 17 (2009) 2524–2535.
- [14] N.A. Colabufo, F. Berardi, M. Cantore, M.G. Perrone, M. Contino, C. Inglese, M. Niso, R. Perrone, A. Azzariti, G.M. Simone, L. Porcelli, A. Paradiso, *Bioorg. Med. Chem.* 16 (2008) 362–373.
- [15] N.A. Colabufo, F. Berardi, M. Cantore, M.G. Perrone, M. Contino, C. Inglese, M. Niso, R. Perrone, A. Azzariti, G.M. Simone, A. Paradiso, *Bioorg. Med. Chem.* 16 (2008) 3732–3743.
- [16] G. Zhu, J. Gong, A. Claiborne, K.W. Woods, V.B. Gandhi, S. Thomas, Y. Luo, X. Liu, Y. Shi, R. Guan, S.R. Magnone, V. Klinghofer, E.F. Johnson, J. Bouska,

- A. Shoemaker, A. Oleksijew, V.S. Stoll, R. De Jong, T. Oltersdorf, Q. Li, S.H. Rosenberg, V.L. Giranda, *Bioorg. Med. Chem. Lett.* 16 (2006) 3150–3155.
- [17] B. Lei, L. Xi, J. Li, H. Liu, X. Yao, *Anal. Chim. Acta* 644 (2009) 17–24.
- [18] M. Cushman, M. Jayaraman, J.A. Vroman, A.K. Fukunaga, B.M. Fox, G. Kohlhausen, D. Strumberg, Y. Pommier, *J. Med. Chem.* 43 (2000) 3688–3698.
- [19] A. Ioanoviciu, S. Antony, Y. Pommier, B.L. Staker, L. Stewart, M. Cushman, *J. Med. Chem.* 48 (2005) 4803–4814.
- [20] X. Xiao, S. Antony, Y. Pommier, M. Cushman, *J. Med. Chem.* 48 (2005) 3231–3238.
- [21] A. Morrell, M.S. Placzek, J.D. Steffen, S. Antony, K. Agama, Y. Pommier, M. Cushman, *J. Med. Chem.* 50 (2007) 2040–2048.
- [22] M. Nagarajan, A. Morrell, B.C. Fort, M.R. Meckley, S. Antony, G. Kohlhausen, Y. Pommier, M. Cushman, *J. Med. Chem.* 47 (2004) 5651–5661.
- [23] M. Nagarajan, A. Morrell, A. Ioanoviciu, S. Antony, G. Kohlhausen, K. Agama, M. Hollingshead, Y. Pommier, M. Cushman, *J. Med. Chem.* 49 (2006) 6283–6289.
- [24] M. Nagarajan, X. Xiao, S. Antony, G. Kohlhausen, Y. Pommier, M. Cushman, *J. Med. Chem.* 46 (2003) 5712–5724.
- [25] M. Nagarajan, A. Morrell, S. Antony, G. Kohlhausen, K. Agama, Y. Pommier, P.A. Ragazzon, N.C. Garbett, J.B. Chaires, M. Hollingshead, M. Cushman, *J. Med. Chem.* 49 (2006) 5129–5140.
- [26] H.T.M. Van, Q.M. Le, K.Y. Lee, E.-S. Lee, Y. Kwon, T.S. Kim, T.N. Le, S.-H. Lee, W.-J. Cho, *Bioorg. Med. Chem. Lett.* 17 (2007) 5763–5767.
- [27] X. Xiao, S. Antony, G. Kohlhausen, Y. Pommier, M. Cushman, *Bioorg. Med. Chem. Lett.* 12 (2004) 5147–5160.
- [28] E.M. Doherty, C. Fotsch, A.W. Bannon, Y. Bo, N. Chen, C. Dominguez, J. Falsey, N.R. Gavva, J. Katon, T. Nixey, V.I. Ognyanov, L. Pettus, R.M. Rzasa, M. Stec, S. Surapaneni, R. Tamir, J. Zhu, J.J.S. Treanor, M.H. Norman, *J. Med. Chem.* 50 (2007) 3515–3527.
- [29] J.A. Christopher, P. Bamborough, C. Alder, A. Campbell, G.J. Cutler, K. Down, A.M. Hamadi, A.M. Jolly, J.K. Kerns, F.S. Lucas, G.W. Mellor, D.D. Miller, M.A. Morse, K.D. Pancholi, W. Rumsey, Y.E. Solanke, R. Williamson, *J. Med. Chem.* 52 (2009) 3098–3102.
- [30] D.V. Kravchenko, Y.A. Kuzovkova, V.M. Kysil, S.E. Tkachenko, S. Maliarchouk, I.M. Okun, K.V. Balakin, A.V. Ivachtchenko, *J. Med. Chem.* 48 (2005) 3680–3683.
- [31] R. Anand, J. Maksimoska, N. Pagano, E.Y. Wong, P.A. Gimotty, S.L. Diamond, E. Meggers, R. Marmorstein, *J. Med. Chem.* 52 (2009) 1602–1611.
- [32] I. Ortín, J.F. González, E. de la Cuesta, C. Manguan-García, R. Perona, C. Avendaño, *Bioorg. Med. Chem.* 16 (2008) 9065–9078.
- [33] K. Charupant, N. Daikuhara, E. Saito, S. Amnuoyopol, K. Suwanborirux, T. Owa, N. Saito, *Bioorg. Med. Chem.* 17 (2009) 4548–4558.
- [34] J.A. Kaizerman, M.I. Gross, Y. Ge, S. White, W. Hu, J.-X. Duan, E.E. Baird, K.W. Johnson, R.D. Tanaka, H.E. Moser, R.W. Bürli, *J. Med. Chem.* 46 (2003) 3914–3929.
- [35] A. Opitz, E. Roemer, W. Haas, H. Görls, W. Werner, U. Gräfe, *Tetrahedron* 56 (2000) 5147–5155.
- [36] I. Antonini, R. Volpini, D.D. Ben, C. Lambertucci, G. Cristalli, *Bioorg. Med. Chem.* 16 (2008) 8440–8446.
- [37] L.B. Hendry, V.B. Mahesh, E.D. Bransome Jr., D.E. Ewing, *Mutat. Res.* 623 (2007) 53–71.
- [38] A. Kamal, R. Ramu, V. Tekumalla, G.B.R. Khanna, M.S. Barkume, A.S. Juvekar, S.M. Zingde, *Bioorg. Med. Chem.* 16 (2008) 7218–7224.
- [39] X. Bu, L.W. Deady, G.J. Finlay, B.C. Baguley, W.A. Denny, *J. Med. Chem.* 44 (2001) 2004–2014.
- [40] E. Sperlinga, P. Kosson, Z. Urbanczyk-Lipkowska, G. Ronsisvalle, D.B. Carr, A.W. Lipkowski, *Bioorg. Med. Chem. Lett.* 15 (2005) 2467–2469.
- [41] G. Lesma, E. Meschini, T. Recca, A. Sacchetti, A. Silvani, *Tetrahedron* 63 (2007) 5567–5578.
- [42] S. Liljequist, G. Cebers, A. Kaldas, *Biochem. Pharmacol.* 50 (1995) 1761–1774.
- [43] Y.-F. Zhu, K. Wilcoxon, T. Gross, P. Connors, N. Strack, R. Gross, C.Q. Huang, J.R. McCarthy, Q. Xie, N. Ling, C. Chen, *Bioorg. Med. Chem. Lett.* 13 (2003) 1927–1930.
- [44] A. Cappelli, G.P. Mohr, G. Giuliani, S. Galeazzi, M. Anzini, L. Mennuni, F. Ferrari, F. Makovec, E.M. Kleinrath, T. Langer, M. Valoti, G. Giorgi, S. Vomero, *J. Med. Chem.* 49 (2006) 6451–6464.
- [45] M. Zhao, L. Bi, W. Wang, C. Wang, M. Baudy-Floc'h, J. Ju, S. Peng, *Bioorg. Med. Chem.* 14 (2006) 6998–7010.
- [46] J. Liu, G. Cui, M. Zhao, C. Cui, J. Ju, S. Peng, *Bioorg. Med. Chem.* 15 (2007) 7773–7778.
- [47] A.R. Shaikh, M. Ismael, C.A.D. Carpio, H. Tsuboi, M. Koyama, A. Endou, M. Kubo, E. Broclawick, A. Miyamoto, *Bioorg. Med. Chem. Lett.* 16 (2006) 5917–5925.
- [48] M.R. Doddareddy, Y.S. Cho, H.Y. Koh, A.N. Pae, *Bioorg. Med. Chem.* 12 (2004) 3977–3985.
- [49] R.P. Queiroz, M.S.E. Castanheir, C.T.T. Lopes, K.Y. Cruz, G. Kirsch, *J. Photochem. Photobiol. A* 190 (2007) 45–52.